nature food

Article

https://doi.org/10.1038/s43016-026-01302-7

Winter wheat yield sensitivity to snow drought is increasing across the Northern Hemisphere

Received: 19 August 2024

Accepted: 9 January 2026

Published online: 06 February 2026

Check for updates

Huijiao Chen [1], Shuo Wang [1,2] ✉, Peng Zhu [3] & Amir AghaKouchak [4,5,6]

Global crop productivity heavily relies on snow availability, which has declined in many snow-dependent regions due to warmer winters and intensified snow droughts. However, our understanding of crop yield sensitivity to snow droughts remains limited. Here we show that winter wheat croplands have experienced an increase in snow drought frequency (5.3–6.7% more events per decade) from 1960 to 2020. To assess the sensitivity of winter wheat yield to snow droughts, we utilized explainable machine learning, gridded yield datasets and the standardized snow water equivalent index from 1982 to 2016. Our findings reveal a significant increase in yield sensitivity to snow water equivalent index over 25% of Northern Hemisphere winter wheat croplands. Elevated fertilizer application rates, increased freezing stress and slightly decreased precipitation are identified as primary drivers amplifying this sensitivity. These findings highlight the increasing vulnerability of crop systems to snow droughts, which is critical for guiding agricultural adaptation in a warming future with reduced snowpack.

Snowpack provides critical water resources to human societies and ecosystems[1], playing a key role in sustaining overwintering crop production[2–5]. Recent observations have highlighted an increasing shift in cold-season precipitation from snow to rain[1], resulting in a decrease in snowpack. This shift has garnered notable attention from researchers, practitioners and policymakers, particularly in regions experiencing extremely low snowpack[6,7]. A notable instance occurred during the winter of 2014/2015, when the western USA experienced widespread, record-low snowpack, a phenomenon referred to as a snow drought[6]. This snow drought resulted in a loss of US$850 million in crop revenue and over 18,600 jobs in California[8]. Moreover, the subsequent winter of 2020/2021 further underscored the region's vulnerability to snow drought, exacerbating the ongoing warm-season drought of 2020[9]. Similar events have been observed in many countries around the world. Afghanistan faced a snow drought in the winter of 2017/2018, contributing to crop failures and food insecurity for over 10.6 million people[10]. European countries have also experienced snow droughts[11]. These cases underscore the global threat that snow droughts pose to food security[12].

Snow droughts pose a triple threat to overwintering crop production, including a reduction in the insulation of soil and early vegetation[4], a reduction in the amount of snowmelt runoff[13] and groundwater available for irrigation[2,14] and an increased risk of agricultural droughts in the following warm seasons[7]. Field studies and model simulations have shown that decreased snow cover might compromise the insulation of crops such as winter wheat against frost and freeze[4,6], particularly during ear emergence and early crop growth. Moreover, a lower snowmelt rate may reduce the amount of meltwater reaching croplands, leading

[1]State Key Laboratory of Climate Resilience for Coastal Cities, Department of Land Surveying and Geo-Informatics, The Hong Kong Polytechnic University, Hong Kong, China. [2]Otto Poon Research Institute for Climate-Resilient Infrastructure and Research Institute for Land and Space, The Hong Kong Polytechnic University, Hong Kong, China. [3]Department of Geography, The University of Hong Kong, Hong Kong, China. [4]Department of Civil and Environmental Engineering, University of California, Irvine, Irvine, CA, USA. [5]Department of Earth System Science, University of California, Irvine, Irvine, CA, USA. [6]United Nations University Institute for Water, Environment and Health, Richmond Hill, Ontario, Canada. ✉e-mail: shuo.s.wang@polyu.edu.hk

to insufficient agricultural water for later crop growth[3,13,15], especially in regions such as the western USA where agricultural water availability relies heavily on snowmelt[6,7]. Furthermore, earlier snowmelt during the winter and early spring may exacerbate the challenges of hotter and drier summers owing to the absence of snowmelt runoff[13–15]. There is strong theoretical, model-based and empirical evidence that snow droughts will increase in a warming climate[16]. However, no global studies have comprehensively analysed the risk that snow droughts pose to overwintering crop yield, even though the dependence of crop production on snowmelt has long been recognized as a key climate change risk[12,17].

Winter wheat, a particularly snow-dependent crop[2], is the major cereal crop grown globally. In this study, we first investigate the hotspots and trends of snow drought across winter wheat croplands during the period of 1960–2020, based on the standardized snow water equivalent index (SWEI) derived from the ERA5-Land[18] and Global Land Data Assimilation System (GLDAS) datasets[19]. In addition, we examine the sensitivity of winter wheat yield to SWEI and changes in yield sensitivity to SWEI for the period of 1982–2016. We also explore the underlying mechanisms driving the increasing sensitivity of yield to SWEI. Our findings reveal a growing risk of snow drought in winter wheat croplands and an increased sensitivity of winter wheat yield to snow drought over the past 30 years, a trend that existing research has overlooked.

Hotspots and trends of snow drought across winter wheat croplands

Before assessing the impact of snow droughts on crop yields, we examined changes in the frequency of snow droughts across winter wheat croplands. The SWEI was estimated using a 3-month sum of daily snow water equivalent (SWE) for the months of January, February and March (JFM), providing a reliable approximation of annual snowpack dynamics[6,16]. A threshold of −1 for the SWEI represents a SWE anomaly of less than or equal to one standard deviation under drought conditions. A threshold of −0.8 for the SWEI was selected[6] to ensure a sufficient number of events for reliable estimation of snow droughts (Methods). The snow drought frequency was calculated based on 10-year or 15-year blocks.

We identified spatial patterns of snow drought frequency across the Northern Hemisphere's winter wheat croplands (Fig. 1a), highlighting frequent occurrences in the USA, Europe, Central Asia and Eastern Asia, with peaks of three to four events per decade. Between 1960 and 2020, snow drought frequency shows a significant increase (5.3–6.7% more events per decade, $P < 0.05$) across the USA, Europe, Central Asia and Eastern Asia (Fig. 1b–e). Therefore, our study focused on these four crucial wheat-producing and snow-dependent regions, collectively accounting for 77% of the total winter wheat yield globally from 1982 to 2016. Any major winter wheat yield loss in these regions could critically affect global food trade and food security[20]. In addition, the proportion of croplands exposed to snow drought shows a significant increasing trend ($P < 0.001$) across the Northern Hemisphere (NH), including the USA, Europe, Central Asia and Eastern Asia (Fig. 1f). This proportion increased from approximately 46–54% during the period of 1960–1970 to approximately 70–99% during the period of 2010–2020 (Fig. 1f). Overall, approximately 49% of winter wheat croplands show a significant upward trend in snow drought frequency (Fig. 1g). The results show a consistent trend for the alternative GLDAS dataset (Fig. 1g and Supplementary Fig. 1). We also conducted analyses using different thresholds of SWEI ($R^2 = 0.96$; Supplementary Fig. 2) and different sizes of moving blocks ($R^2 = 0.72$; Supplementary Fig. 3) to verify the robustness of the observed increases in snow drought frequency.

As a representative region, the western USA, identified as particularly susceptible to snow droughts, experienced remarkable snow drought events from the winter of 2014/2015 (Supplementary Fig. 4). Consequently, severe water shortages in the summer of 2015 reduced agricultural production, forced the fallowing of 564,000 acres of cropland and contributed to the loss of 8,550 direct farm jobs in California[8]. Analysis of snow drought frequency over winter wheat croplands provides crucial insights into the risk that warmer winters pose to overwintering food production. This observed increase in snow drought frequency is consistent with previous findings[6,8,11,16] and reveals an emerging influence of climate warming on snow drought impacts in agricultural systems.

Sensitivity of winter wheat yield to SWEI

To evaluate the impacts of snow anomalies on winter wheat yield variability, we applied convergent cross mapping (CCM)[21] and the nonlinear Granger causality test[22] to investigate the causal mechanisms between snow and crop yield. CCM is a powerful tool for conducting causal inference between winter wheat yield and SWEI, as it accounts for confounding factors within complex ecosystems. Our results (Supplementary Fig. 5) reveal that the skill level in cross mapping from winter wheat yield to SWEI, with a Pearson correlation coefficient ($\rho = 0.31$, not statistically significant with $P > 0.05$), is much lower than that from SWEI to winter wheat yield ($\rho = 0.51$, statistically significant with $P < 0.001$). The winter wheat cropland exhibits clear Granger causality between SWEI and yield dynamics (Supplementary Fig. 6). These findings suggest that snow dynamics contribute to yield anomalies in winter wheat production.

To better understand the impact of snow drought on crop yield, we used the Shapley additive explanations (SHAP)[23] within Extreme Gradient Boosting (XGBoost) models[24] (Methods and Supplementary Fig. 7). This framework enabled us to isolate the contribution of SWEI to winter wheat yield anomalies, distinguishing it from the influence of other climate extremes (Supplementary Table 1). To explore regional variability in the snow–crop relationship, we built four distinct XGB-SHAP models for four snow cover croplands: the USA, Europe, Central Asia and Eastern Asia. The SHAP values demonstrated a nonlinear relationship with the SWEI across the four key croplands (Fig. 2a–d). A larger negative SHAP value indicates a higher probability of yield loss, and vice versa. We conducted a comprehensive analysis of the sensitivity of winter wheat yield to SWEI from 1982 to 2016. Sensitivity is defined as the slope estimated from the piecewise linear approach[25] between SHAP values and SWEI, with a breakpoint at SWEI of 0, indicating the effects of snow drought on yield anomalies. A significantly ($P < 0.05$) positive sensitivity indicates that decreases in SWEI suppress winter wheat yield.

Under snow drought conditions (SWEI ≤ −0.8), the correlation between SHAP and SWEI was nearly positive (Fig. 2a–c), indicating that winter wheat yield decreased with more severe snow drought across the USA (63%), Europe (62%) and Central Asia (57%). Conversely, Eastern Asia exhibited more diverse effects, with approximately 85% of points experiencing opposite relationships. Figure 2i shows that the area fraction of croplands with positive overall sensitivity is higher than those with negative overall sensitivity across Northern Hemisphere croplands. Specifically, approximately 45% of Northern Hemisphere croplands experienced a significantly ($P < 0.05$) adverse impact from snow droughts, with the effects primarily concentrated in the USA (41%), Europe (53%) and Central Asia (50%). The detrimental effects of lower SWEI on yield underscore the substantial impact of snow drought stress, driven primarily by extreme heat and declining precipitation[15]. However, the effect of snow drought on winter wheat yield in Eastern Asia is reversed compared with the other three major winter wheat regions (Fig. 2a–h). This reversal is primarily attributed to the cropland's lower cumulative snowpack (Supplementary Fig. 8), which minimizes the roles of snowpack insulation and water supply for winter wheat production. Moreover, field experiments and grid-based simulations in China indicate that warmer winters can increase yields by shortening dormancy and the pre-anthesis period, extending grain filling and enhancing photosynthesis through earlier leaf development[26]. By contrast, the other three regions rely on thicker snowpack for insulation

https://doi.org/10.1038/s43016-026-01302-7

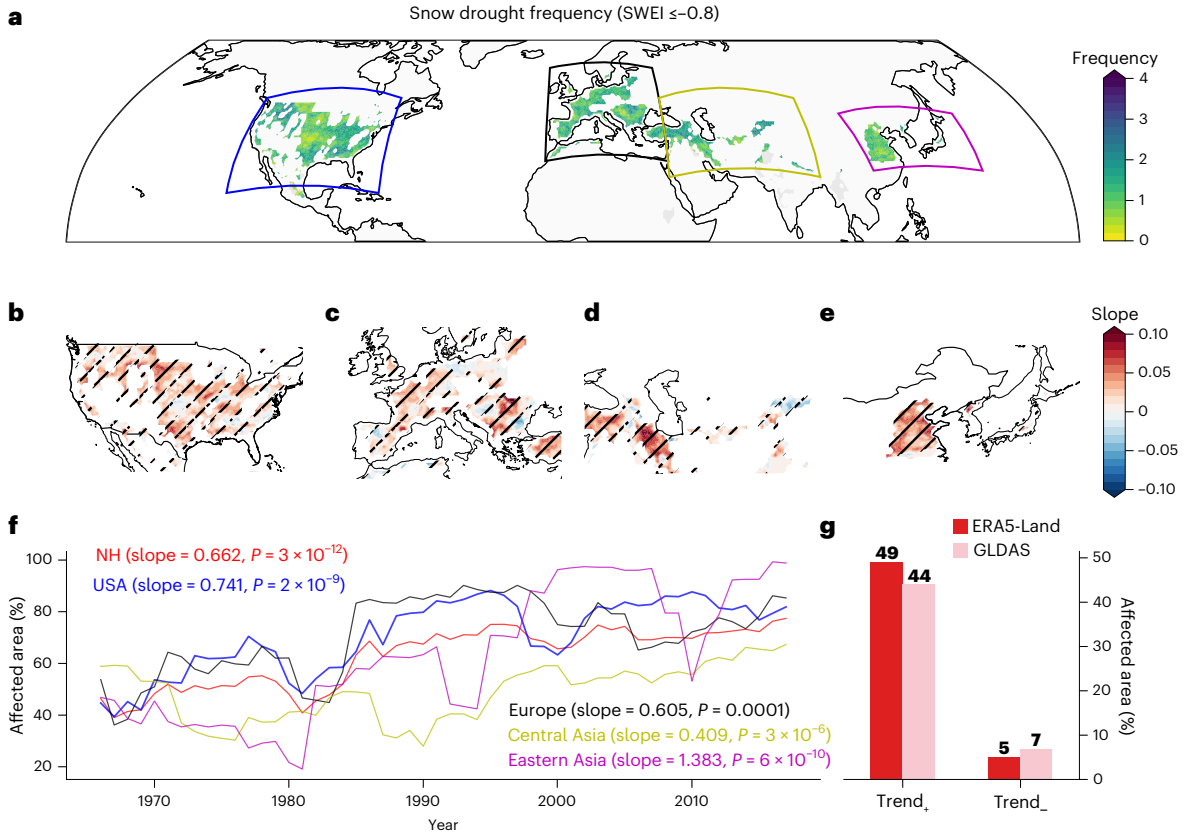

Fig. 1 | Hotspots and trends in snow drought frequency. a, The spatial distribution of the decadal sum of snow drought frequency during 1960–2020. **b**–**e**, The spatial distribution of the slope (events per decade) of trends in snow drought frequency for the USA (**b**), Europe (**c**), Central Asia (**d**) and Eastern Asia (**e**). The slope was estimated using Theil–Sen regression. Statistical significance was evaluated using a two-sided Mann–Kendall test. *P* values were adjusted for multiple comparisons using the Benjamini–Hochberg false discovery rate procedure. Stippling indicates areas where the trend is statistically significant (adjusted $P < 0.05$). **f**, The temporal evolution of the snow drought-affected area of croplands (%) using 10-year blocks. The numbers represent the slope (% per decade) of trends in snow drought-affected croplands by the Theil–Sen regression. Statistical significance was evaluated using a two-sided Mann–Kendall test. **g**, The proportion of croplands (%) with increasing trends ($Trend_+$) and decreasing trends ($Trend_-$) in snow drought frequency based on ERA5-Land and GLDAS datasets, with statistical significance at the level of 0.05. Maps in **a**–**e** generated using Cartopy with Natural Earth shapefiles.

(Supplementary Fig. 8). In these contexts, warming increases freeze–thaw stress while reducing the protective snow cover[4,27], leading to larger yield losses during snow drought.

The XGBoost model's performance was estimated by time-series cross-validation (Supplementary Table 2), indicating that 62–72% of the variation in winter wheat yields can be explained by variations in climate extremes in the USA, Europe and Eastern Asia. In Central Asia, only 41% of the yield variation can be explained by these climatic factors owing to grid points having 71% of missing data (Supplementary Table 3). The results of December, January and February SWEI and JFM SWEI show agreements in their spatial patterns (Supplementary Fig. 9) and a strong correlation ($R^2 = 0.83$) across Eastern Asia's croplands (Supplementary Fig. 10), indicating the robustness of snow drought effects on overwintering crop production.

Increasing sensitivity of winter wheat yield to SWEI

To assess the temporal variation in snow drought effects, we analysed the sensitivity of yield to SWEI by 10-year blocks spanning from 1982 to 2016. The sensitivities of yield to SWEI fluctuated across the moving block time series, with slopes estimated using a piecewise linear approach with a breakpoint at SWEI of 0. These temporally varying sensitivities were represented as the trend in sensitivity (T_{sen}; Methods and Supplementary Fig. 7). We defined an increasing trend in the sensitivity of yield to SWEI (T_{sen+}) as cases where the sensitivity shows a significant ($P < 0.05$) increase from 1982 to 2016, indicating more pronounced impacts of snow droughts on yields. Conversely, a decreasing trend in the sensitivity of yield to SWEI (T_{sen-}), suggesting a diminishing impact of snow droughts over time.

During the period from 1982 to 2016 in the Northern Hemisphere croplands, we observed a significant increase in T_{sen} (slope of 0.034 t ha^{-1} mm^{-1} decade^{-1}, $P < 0.001$; Fig. 3a). The sensitivity increased from 0.4 ± 1.05 to 0.8 ± 1.45 t ha^{-1} mm^{-1} from the initial to the final moving window. We also observed escalating T_{sen} over four key winter wheat-producing regions (Fig. 3c–f), with a slope of 0.023 ($P < 0.001$) for croplands in the USA, a slope of 0.077 ($P < 0.001$) for croplands in Europe, a slope of 0.195 ($P = 0.001$) for croplands in Central Asia and a slope of 0.113 ($P = 0.036$) for croplands in Eastern Asia. Across the Northern Hemisphere croplands, the proportions for T_{sen+} and T_{sen-} were 25% and 9%, respectively. This indicates a prevalence of croplands with increasing sensitivity over those with decreasing sensitivity. Specifically, the proportions for T_{sen+} and T_{sen-} were 24% and 15%, respectively, across the USA. Overall, a significant increase in yield sensitivity to SWEI was found in approximately 25% of winter wheat croplands, primarily concentrated across western and southern USA, northern and southeastern Europe (40%), western Asia (18%) and northern China (18%) (Fig. 3g–j).

We validated the robustness of our results by (1) repeating the analysis using 15-year blocks (Supplementary Fig. 11), (2) testing the analysis with an alternative GLDAS dataset (Supplementary Fig. 12)

https://doi.org/10.1038/s43016-026-01302-7

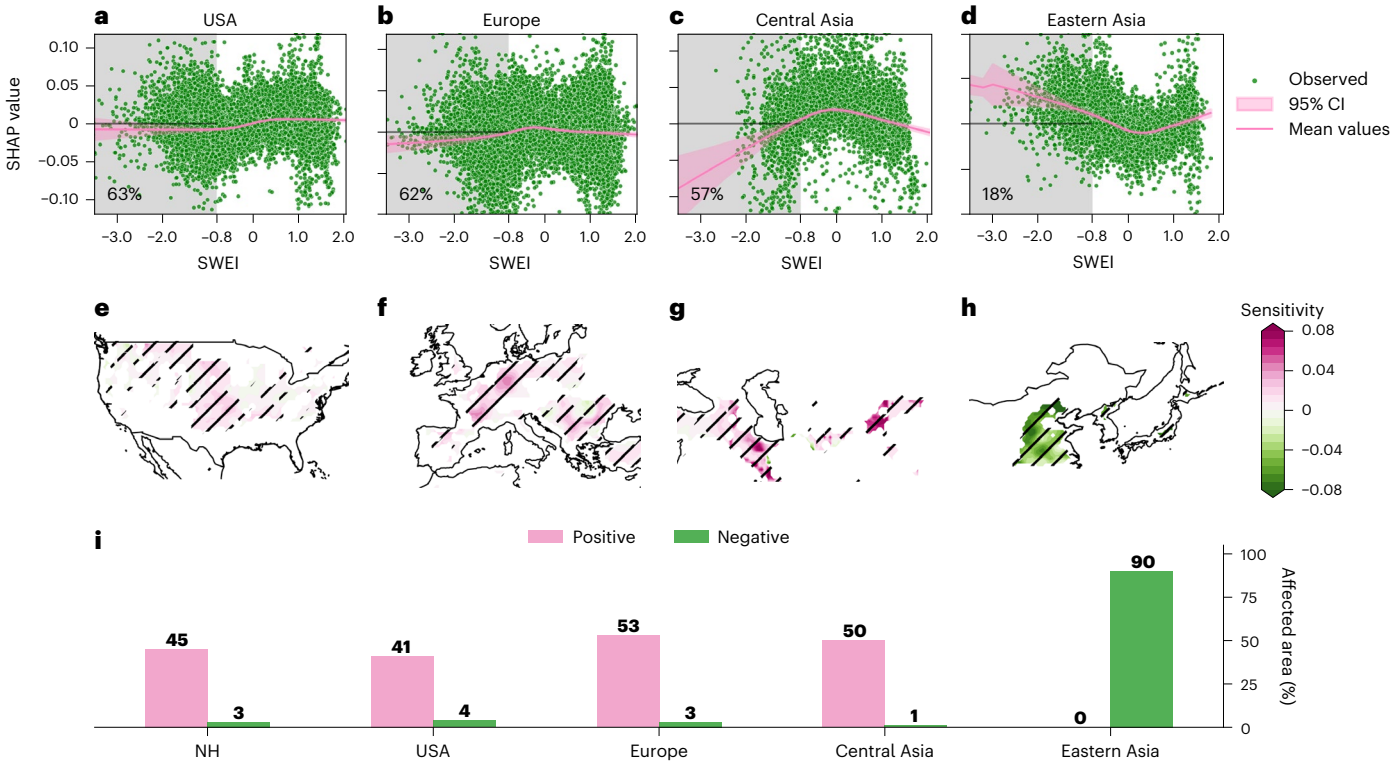

Fig. 2 | The overall sensitivity of winter wheat yield to snow droughts from 1982 to 2016. a–**d**, Response curves for yield response to SWEI generated through partial dependence plot using the XGB-SHAP framework (Methods), for the USA (**a**), Europe (**b**), Central Asia (**c**) and Eastern Asia (**d**). A larger negative SHAP value indicates a higher probability of yield loss, and vice versa. The lower and upper bounds of the pink shading represent the 2.5th and 97.5th percentile estimates (95% confidence interval (CI)), respectively. The shaded grey area represents snow drought conditions (SWEI ≤–0.8). The numbers indicate the proportion of grid points within the shaded grey area. **e**–**h**, The spatial distribution of overall sensitivity for the USA (**e**), Europe (**f**), Central Asia (**g**) and Eastern Asia (**h**). In **e**–**h**, the sensitivity was estimated using a piecewise linear regression model and statistical significance was assessed using two-sided tests with *P* values derived from the regression model. To account for multiple comparisons across grid cells, *P* values were adjusted using the Benjamini–Hochberg false discovery rate procedure. Stippling indicates areas where the sensitivity is statistically significant (adjusted $P < 0.05$). **i**, The proportion of croplands with (pink) positive sensitivity and (green) negative sensitivity, based on adjusted $P < 0.05$. Maps in **e**–**h** generated using Cartopy with Natural Earth shapefiles.

and (3) using an alternative tree-based random forest machine learning method (Supplementary Fig. 13). In all these cases, we found similar results. Moreover, the analysis was conducted at a county level across the USA winter wheat croplands using an observational crop yield dataset (USDA NASS database)[28]. The results obtained with the observational winter wheat yield data were consistent (Supplementary Figs. 14–16). Overall, our findings from two independent snow datasets, two machine learning methods and two winter wheat yield datasets suggest an increased impact of snow droughts on wheat yields over the past three decades in key winter wheat-producing regions.

Attribution of sensitivity trends

We conducted an attribution analysis (Methods) to understand the changes in T_{sen}, which can be explained by the trends of relevant hydroclimatic variables across the winter wheat growing season and human management practices (Supplementary Table 4). The relevant hydroclimatic variables include air temperature (*T*), precipitation (Pre), vapour pressure deficit (VPD), soil moisture (SM) and climate extreme indices across the growing seasons for winter wheat. Human management practices include irrigation ratios, fertilizer application rates (nitrogen, phosphorus and potassium) and variations in soil types (sand and clay).

Our findings reveal that these factors collectively explain 48–74% of the spatial variability in T_{sen} (Fig. 4). We focused on the five most important drivers of sensitivity trends across these four croplands. We categorized regions with significantly ($P < 0.05$) enhanced and weakened yield sensitivity as T_{sen+} and T_{sen-}, respectively. Generally, variations in freezing stress (freezing growing degree days (FDD) and snow cover fraction (SCF)) can lead to a pronounced change in T_{sen} across the USA, Europe and Central Asia (Fig. 4a–c). Higher freezing stress (Supplementary Fig. 17) increases yield sensitivity to snow drought, which might be related to reduced insulation of soil and early crops, resulting in greater exposure to extremely low temperatures[4]. Fertilizer application rates[29] are also critical factors influencing spatial variations of T_{sen} across the four croplands, which can mitigate the effects of snow droughts on yield. In Eastern Asia (Fig. 4d), our results suggest that a small reduction in water moisture (soil moisture and rainfall) could exacerbate the effects of snow droughts on yield.

Snow droughts interact substantially with other hydroclimate variables, potentially resulting in complex effects on winter wheat growth. To understand these interactions, we used a SHAP interaction plot to illustrate the interactive effects of snow conditions and key variables (Fig. 4). In the USA (Supplementary Fig. 18), lower SWEI coupled with reduced SM in fall and winter produced negative SHAP interaction values, indicating a synergistic negative effect on yield. A distinct interactive effect between SWEI and VPD was observed across European croplands (Supplementary Fig. 19). Intensified snow droughts correlated with higher spring VPD, demonstrating a stronger interactive effect than that between snow drought and high spring extreme growing degree days (EDD). In Central Asia, the interactive effects intensified when snow droughts coincided with increased autumn FDD (Supplementary Fig. 20). Conversely, when autumn and winter EDD increased alongside intensified snow droughts, the SHAP interaction value decreased across croplands in Central Asia and Eastern Asia (Supplementary Figs. 20 and 21). Overall, these varied interactive

https://doi.org/10.1038/s43016-026-01302-7

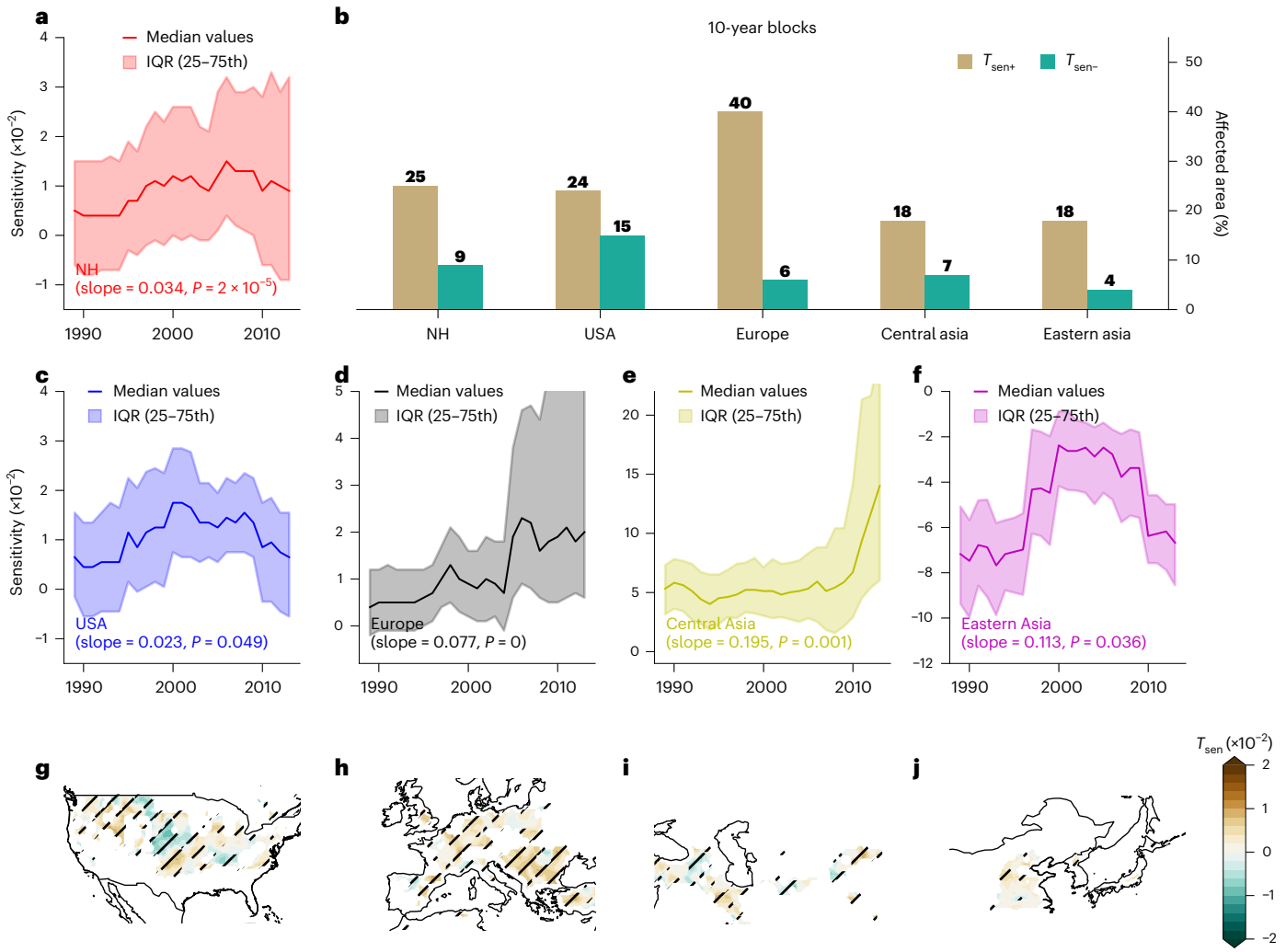

Fig. 3 | Trends in sensitivity of winter wheat yield to SWEI. a, The temporal evolution of winter wheat yield sensitivity to SWEI for the NH. **b**, The proportion of croplands with significantly increasing sensitivity (brown, T_{sen+}) and significantly decreasing sensitivity (cyan, T_{sen-}), based on adjusted $P < 0.05$. **c**–**f**, The temporal evolution of winter wheat yield sensitivity to SWEI for the USA (**c**), Europe (**d**), Central Asia (**e**) and Eastern Asia (**f**). The lower and upper bounds of the shaded area represent the 25th and 75th percentile of sensitivity blocks (IQR 25–75th), respectively. The numbers represent the slope of trends of sensitivity by the Theil–Sen regression and statistical significance was assessed using a two-sided Mann–Kendall test. **g**–**j**, The spatial distribution of trends of sensitivity (T_{sen}) for the USA (**g**), Europe (**h**), Central Asia (**i**) and Eastern Asia (**j**). The sensitivity trends were estimated using Kendall's rank correlation and statistical significance was assessed using two-sided tests with P values derived from the asymptotic normal distribution. P values were adjusted using the Benjamini–Hochberg false discovery rate procedure. Stippling indicates areas where sensitivity is statistically significant (adjusted $P < 0.05$). Maps in **g**–**i** generated using Cartopy with Natural Earth shapefiles.

pathways demonstrate that snow droughts affect winter wheat yield through region- and season-specific mechanisms.

Discussion

To evaluate the implications of snow droughts for crop yields under warming conditions, we utilized the XGB-SHAP framework. This approach can effectively isolate the effect of snow drought on winter wheat yield from other relevant factors, going beyond purely correlation-based analyses. Our findings reveal a significant increase in the frequency of snow droughts, with a slope of 5.3–6.7% more events per decade, across Northern Hemisphere croplands. The sensitivity of yield to snow drought also shows a significant increase, with a slope of 3.4% t ha^{-1} mm^{-1} decade^{-1}. These results indicate that snow droughts threaten winter wheat production by (1) reducing the insulating effects of snow cover and increasing freezing stress[4,5], (2) decreasing soil moisture and water availability during critical growth stages[2,7,13,15], (3) exacerbating challenges from hotter and drier conditions[16] and (4) limiting nitrogen replenishment and reducing soil fertility[30]—all of which collectively contribute to winter wheat yield losses (Fig. 5). This underscores the importance of jointly considering snow variation and across-season cropping systems to better understand changes in the crop–snow interplay. The observed increase in wheat yield sensitivity to snow drought generally highlights heightened ecosystem vulnerability to a low-to-no snow future[31]. By pinpointing regions of pronounced and escalating yield sensitivity, our study identifies the hotspot areas where rising snow drought trends could lead to more severe impacts on overwintering crop yields.

Snow droughts may interact with crop systems, potentially resulting in both positive and adverse effects. On one hand, snow drought occurrences may benefit crop yield by accelerating growth stages and extending the growing season, thereby enhancing productivity. Moreover, the impacts of snow droughts might be mitigated by the migration of croplands over time and space, as warming conditions could create new areas suitable for agriculture[32]. In addition, expansion of irrigation may alleviate crop yield sensitivity. On the other hand, snow droughts can detrimentally affect crop yield by altering soil microenvironments

https://doi.org/10.1038/s43016-026-01302-7

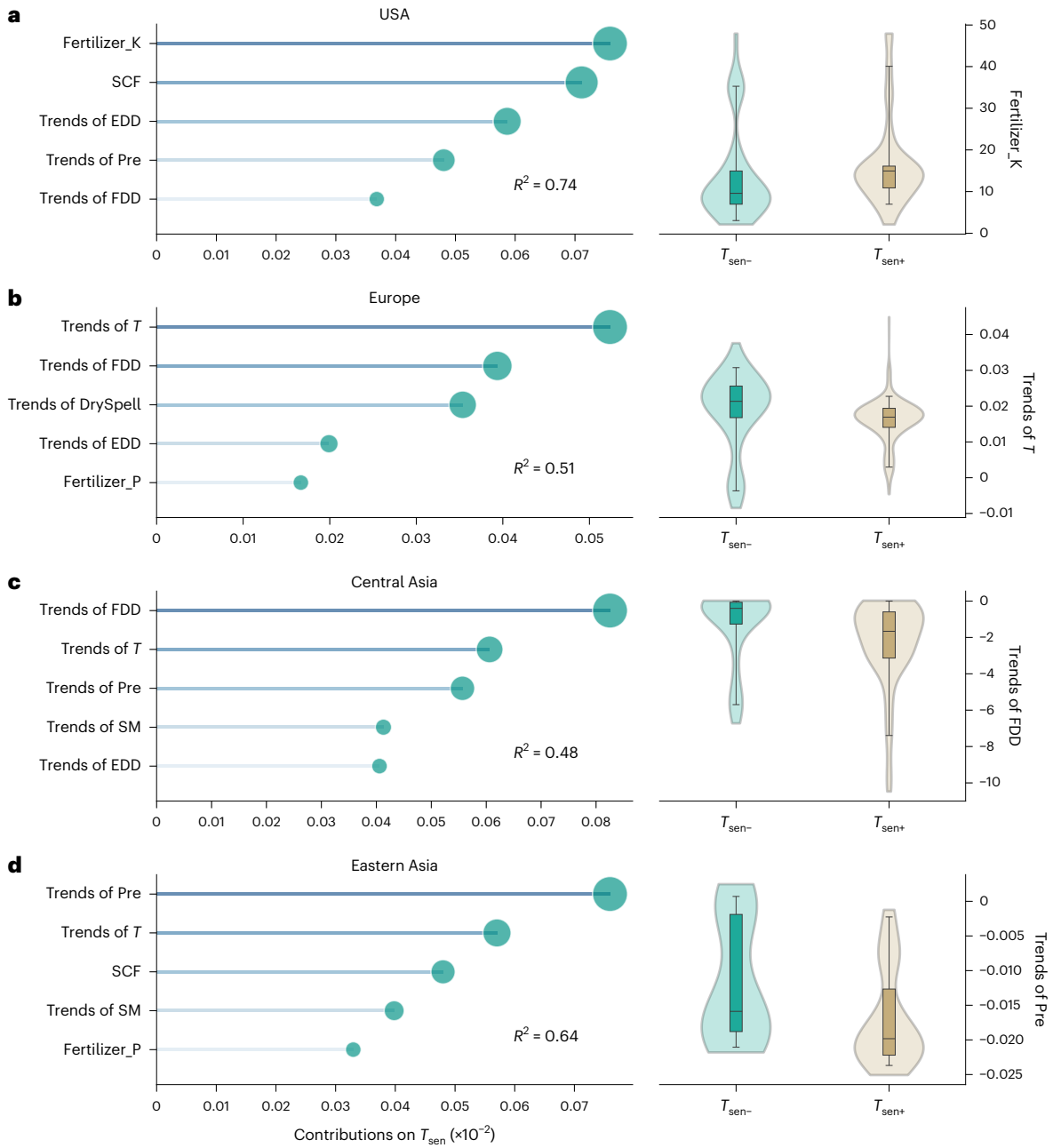

Fig. 4 | The underlying mechanism for the enhanced effects of snow droughts. **a**–**d**, The relative importance and marginal contributions (SHAP values) of multiple predictors to trends in yield sensitivity to SWEI across four cropland areas, including the USA (**a**), Europe (**b**), Central Asia (**c**) and Eastern Asia (**d**), respectively. EDD denotes extreme growing degree days above the optimum temperature thresholds. FDD denotes freezing growing degree days below the freezing growing temperature thresholds. Fertilizer_K and Fertilizer_P denote the potassium and phosphorus fertilizer application rates, respectively. The bar represents the most important drivers of sensitivity trends across four cropland areas. In the box plots, the central line indicates the median; the bottom and top of each box represent the 25th and 75th percentiles, respectively; and the whiskers extend to the 5th and 95th percentiles. Values outside this range are plotted as individual points. R^2 represents the coefficient of determination of the XGBoost model.

and increasing the risk of freezing damage to early crops[4]. In many critical winter wheat production regions, irrigation depends heavily on groundwater, which is potentially replenished by snowmelt; however, large uncertainties remain in quantifying the contribution of snowmelt to groundwater sources[33]. Furthermore, snow droughts are expected to intensify in a warming future[31], exacerbating the risk of water scarcity in many snow-dependent croplands, necessitating alternative sources of agricultural water.

Several limitations of our study should be acknowledged. First, although our analysis spans the full growing season and winter months (JFM), future work could explore the importance of early snowmelt triggered by snow droughts, particularly concerning crop growth phases and springtime variations in soil moisture. Second, owing to the lack of field experiments regarding monthly temperature thresholds for winter wheat in the other three key croplands, we used the same threshold values obtained from North America field data[34]. Finally, other factors such as hail and wind, pests and disease, groundwater and irrigation systems, although not included in our analysis owing to spatial resolution constraints, probably contribute to or mediate yield responses, potentially explaining regional variations.

To mitigate the negative impacts of snow drought on yields, several practical agricultural adaptation measures can be implemented.

https://doi.org/10.1038/s43016-026-01302-7

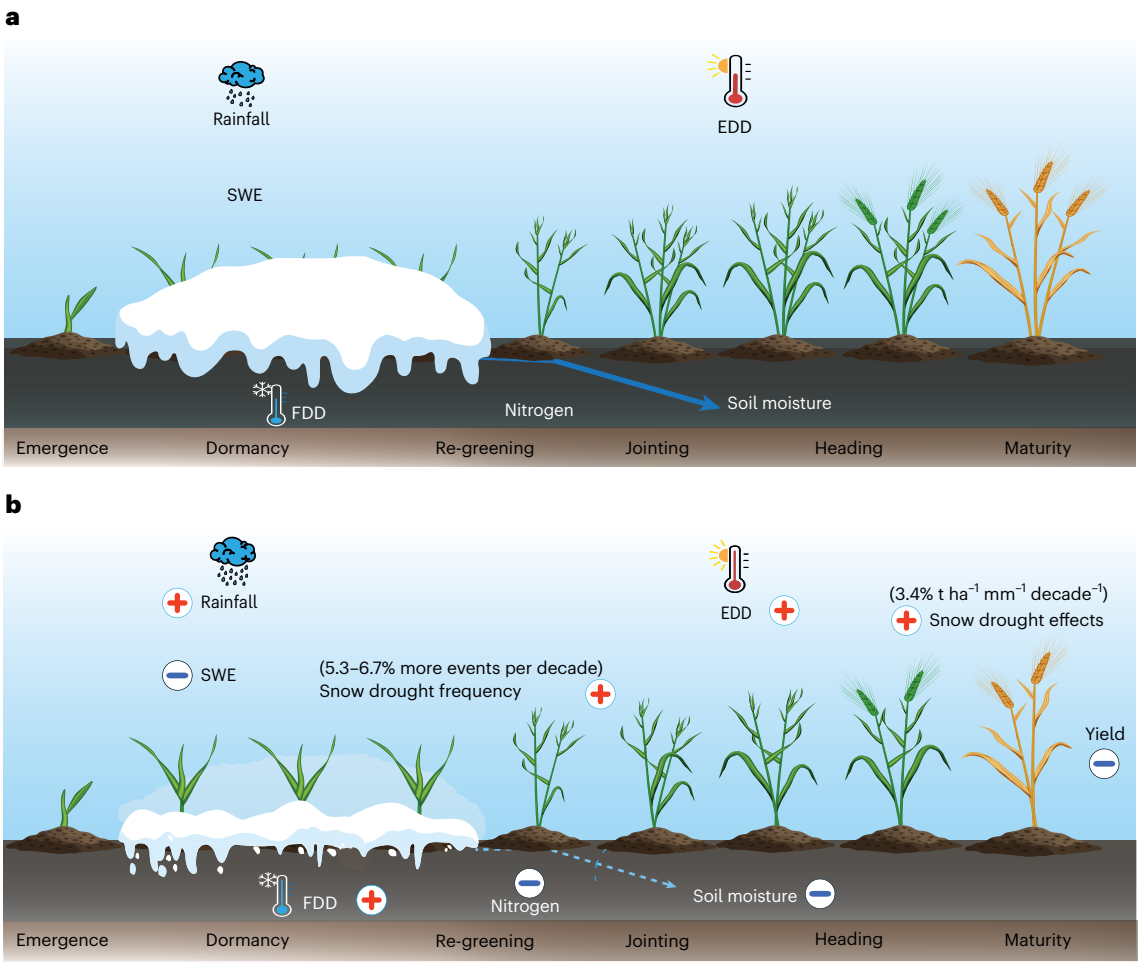

Fig. 5 | Schematic diagram illustrating the impact of snow droughts on winter wheat yields. a, Normal snowpack conditions. **b**, Snow drought conditions. The symbols ⊕ and ⊖ indicate increasing and decreasing changes in variables, respectively. Credit: icons, Freepik.com.

First, establishing snow drought monitoring systems is essential for early detection and management. Second, developing early warning systems will enable farmers to prepare for incoming snow droughts. These systems can provide forecasts and alerts, allowing farmers to make informed decisions about planting and irrigation schedules[35]. For regions reliant on snowmelt for irrigation, adaptive strategies such as investing in efficient irrigation technologies and exploring alternative water sources are critical to offset reduced snowmelt availability. Finally, investing in research to develop wheat varieties resistant to freezing and heat stress is vital. These improved varieties can enhance crop resilience to climate variability and help ensure stable yields under adverse conditions.

Linking snow drought information to agriculture systems is particularly important in crop-producing countries, where the impacts of snow drought can propagate globally through trade networks and exacerbate food insecurity[12]. Snow exhibits substantial sensitivity to different levels of future warming. For this reason, snow droughts are projected to become increasingly frequent[7] due to warming winters, with escalating impacts on crop growth (Fig. 3). However, these impacts may not be uniform across all regions, with some croplands experiencing notable water availability implications while others remain relatively unaffected. Understanding and managing differential vulnerabilities is crucial for comprehending the implications of snow droughts on crop production. Such insights, informed by comprehensive analyses that consider various sources of uncertainty, including datasets and definition choices, are essential for developing efficient and effective adaptations to a less snowy future. Assessing the influences of snow droughts on crop systems represents a critical step towards informed decision-making and resource management in agriculture.

Methods

Yield data

To estimate the crop exposure to snow droughts, we used the Global Dataset of Historical Yield (GDHY)[36] for winter wheat yields, assessing its sensitivity to snow drought. The GDHY dataset provides gridded winter wheat yields for the period of 1982–2016, with a spatial resolution of 0.5°. Comprising agricultural census statistics and satellite remote sensing, the GDHY dataset has been widely used as a primary source in recent global crop–climate studies[37]. To enhance the robustness of the sensitivity of winter wheat yield to snow droughts, we also used an alternative winter wheat yield dataset at a county level, obtained from the USDA NASS QuickStats[38] for the period of 1980–2023.

Phenology data

Winter wheat is typically planted in the autumn, followed by a dormancy period during winter, regrowth in early spring and harvest in the subsequent summer. We collected accurate phenology data (Supplementary Fig. 22) from regional sources and published literature for the USA (USDA NASS QuickStats data), France[39], Germany[40] and China[41]. Together, these regions account for approximately 67% of global winter wheat croplands; the remaining 33% is primarily located in Central Asia and Southern Europe. As phenological stage names and definitions vary between datasets (Supplementary Table 5), we used the

Biologische Bundesanstalt, Bundessortenamt and Chemical Industry (BBCH) scale, an internationally recognized system for crop development stages, to standardize the phenological data[42]. For each region, we summarized the timing of key phenological stages and matched them to the corresponding BBCH codes (Supplementary Table 5). BBCH 30 marks the end of overwintering and the start of re-greening, which typically occurs from late March to early April in most croplands. For Central Asia, where phenological observations are lacking, we used the timing of re-greening phase from the other three regions. Therefore, results for Central Asia should be interpreted with caution, and we emphasize the need for expanded field phenology monitoring in this region to improve future assessments.

Data on human management practices

The irrigation ratios for winter wheat were obtained from the SPAM2010 dataset[43], which uses a cross-entropy approach to downscale area and yield data for 42 crops around the year 2010. In addition, gridded fertilizer rates for wheat were obtained from the EARTHSTAT fertilizer application dataset at a spatial resolution of 5 arc-min[44]. This dataset synthesizes subnational statistics globally and derives crop-specific nitrogen application rates by distributing total nitrogen consumption across maps of wheat cropland areas. Soil types were quantified using the percentages of clay, sand and silt, based on the GLDAS dataset[19].

Climate data

Climate data, including hourly 2-m air temperatures (°C), daily precipitation (mm) and monthly VPD (hPa) computed from dew point temperature (°C), were obtained from the ERA5-Land dataset from 1960 to 2020. Daily root-zone SM ($m^3\ m^{-3}$) was obtained from the Global Land Evaporation Amsterdam Model (GLEAM) dataset[45]. The GLEAM datasets are observationally constrained and have been widely used to analyse global and regional soil moisture changes[46].

To assess the impacts of extreme heat stress, extreme freezing stress, dry stress and heavy rainfall on wheat yields under snow drought conditions, we analysed climate extreme events across the growing seasons (autumn, winter and spring) due to their adverse impacts on winter wheat growth[47]. We calculated the cumulative exposures to growing degree days between the base and optimum growth temperature thresholds (GDD, °Cd, equation (1)), EDD (°Cd, equation (2)) above the optimum growing temperature thresholds and FDD (°Cd, equation (3)) below the freezing growing temperature thresholds over the winter wheat growing season. GDDs, EDDs and FDDs are calculated using the following formulas[34]:

$$\mathrm{GDD}=\sum_{h=1}^{N}\mathrm{DD_h};\ \mathrm{DD_h}=\begin{cases}\frac{T_{\mathrm{opt}}-T_{\mathrm{base}}}{24}, & T_{\mathrm{h}}>T_{\mathrm{opt}}\\ \frac{T_{\mathrm{h}}-T_{\mathrm{base}}}{24}, & T_{\mathrm{base}}\le T_{\mathrm{h}}\le T_{\mathrm{opt}}\\ 0, & T_{\mathrm{h}}<T_{\mathrm{base}}\end{cases}\quad(1)$$

$$\mathrm{EDD}=\sum_{h=1}^{N}\mathrm{DD_h};\ \mathrm{DD_h}=\begin{cases}0, & T_{\mathrm{h}}\le T_{\mathrm{opt}}\\ \frac{T_{\mathrm{h}}-T_{\mathrm{opt}}}{24}, & T_{\mathrm{h}}>T_{\mathrm{opt}}\end{cases}\quad(2)$$

$$\mathrm{FDD}=\sum_{h=1}^{N}\mathrm{DD_h};\ \mathrm{DD_h}=\begin{cases}0, & T_{\mathrm{h}}>T_{\mathrm{frez}}\\ \frac{T_{\mathrm{frez}}-T_{\mathrm{h}}}{24}, & T_{\mathrm{h}}\le T_{\mathrm{frez}}\end{cases}\quad(3)$$

where $\mathrm{DD_h}$ represents the hourly degree-day contribution and N is the total number of hours over the accumulation period. The hourly temperature (T_{h}) was obtained from the ERA5-Land and GLDAS datasets, respectively. T_{base} and T_{opt} are the base and optimum growing temperature thresholds, respectively, specific to each growing phase of wheat (Supplementary Table 6). T_{frez} is the temperature causing freeze injury (Supplementary Table 6).

In addition to the snow effect, rainfall acts as an important water supply to affect winter wheat growth. In this study, precipitation was partitioned into rainfall and snow to represent water supply in different forms based on daily temperature using the following empirical model[1]:

$$\mathrm{Rainfall}=\begin{cases}\mathrm{Pre}, T_{\mathrm{d}}>7\ ^{\circ}\mathrm{C}\\ (1-\mathrm{e}^{\left(0.0000858\times(T_{\mathrm{d}}+7.5)^{4.12}\right)})\times\mathrm{Pre}, 7\ ^{\circ}\mathrm{C}\ge T_{\mathrm{d}}\ge -4\ ^{\circ}\mathrm{C}\\ 0, T_{\mathrm{d}}<-4\ ^{\circ}\mathrm{C}.\end{cases}\quad(4)$$

where Pre is daily precipitation (mm) and T_{d} is the average daily air temperature (°C). The uncertainty of rainfall extremes, associated with different snow–rain partitioning models, was evaluated in Supplementary Text 1. To estimate the effects on winter wheat yields due to specific rainfall extremes, we used two extreme rainfall indices (DrySpell and Max.5D Rain)[48] to represent the effects of rainfall deficit and excess on crop yields. The DrySpell (days) is defined as the maximum number of consecutive days with no rainfall in each season. The Max.5D Rain (mm) is defined as the maximum accumulative rainfall in a 5-day period in each season.

Snow data

We identified snow droughts using two datasets: ERA5-Land[18] and GLDAS[19]. ERA5-Land is a global atmospheric reanalysis product produced by the European Centre for Medium-Range Weather Forecasts[18]. The choice to use these reanalysis datasets is owing to their inclusion of the essential snow variable (snow depth water equivalent) for global winter wheat croplands at a daily timescale, enabling a comprehensive and uniform analysis across different regions and seasonal periods[1]. More importantly, the daily SWE of ERA5-Land agrees better with station observations compared with other datasets, making it an ideal dataset to characterize snow droughts[16]. We used the ERA5-Land dataset for our main analysis and assessed the sensitivity of our results with the alternative GLDAS dataset.

Identification of snow drought

We calculated the daily SWE (mm) from 1 October to 31 May for the entire water year 1948–2022, using a 7-day moving window. We then focused the analysis on winter wheat croplands in the Northern Hemisphere during the winter season, particularly for JFM accumulations of daily SWE, to compute the SWEI. This focus is owing to the fact that early April marks the beginning of re-greening phase of winter wheat in most croplands (Supplementary Table 5), serving as a proxy for water supply capability related to winter snow accumulations[7,15].

The SWEI is widely used to assess snowpack extremes[6,16]. We determined the probabilities based on the empirical Gringorten plotting position $P=(i-0.44)/(n+0.12)$ (where P is the probabilities, n is the sample size of the data and i is the rank of the non-zero variable). The ranks are determined using the JFM accumulations of daily SWE for year. We then computed the SWEI by transforming the empirical probability to standard normal distribution. The SWEI thus provides a comprehensive measure of snow balance over consecutive years, facilitating active monitoring of snow droughts (Supplementary Fig. 4). A threshold of −1 for the SWEI represents the SWE anomaly of less than 1 standard deviation under drought conditions. As snow deviated from normal towards drier conditions, the negative impacts of snow anomalies on yield increased as extreme conditions intensified (Supplementary Fig. 23).

Trends in snow drought frequency

Grids with SWEI ≤ −0.8 (or SWEI ≤ −1 in Supplementary Fig. 2) are defined as snow drought-affected croplands, indicating potential impacts on crop growth due to snow deficits. To address temporal variations of snow drought frequency across winter wheat croplands, we split the data from the entire 1960–2020 period into 50 10-year blocks

(1960–1970, 1961–1971 … 2010–2020). We defined the slope of trends in snow drought frequency estimated from the Theil–Sen regression. We then used the Mann–Kendall's test to detect the statistical significance of the trend in snow drought frequency (Fig. 1), which did not require data with a normal distribution.

Data preprocessing

The SWE, snow depth, SM, VPD, Pre and T data, obtained from ERA5-Land, GLDAS, and GLEAM datasets, were re-gridded to the same resolution of 0.5° × 0.5° using the bilinear interpolation. In all experiments and for all hydroclimatic variables, we selected the growing-season data based on the crop calendar dataset[49] for temporal consistency. The winter wheat growing season, defined as the months between September and July, remains consistent within each growth cycle from 1982 to 2016. We aggregated the daily energy-related (that is, VPD and T) values to the growing-season averages and the daily water-related (that is, SM and Pre) values to growing-season sums. Daily SWE data were aggregated using the 3-month (JFM) sum to calculate yearly SWEI to match yearly yield data. Climate extreme indices of GDD, EDD, FDD, DrySpell and Max.5D rain were calculated in autumn, winter and spring, respectively (Supplementary Table 1).

Effective thermal insulation for crops requires a certain snow depth, typically with a threshold of 2 cm (refs. 4,50). We used the classical formula, snow depth = SWE/snow density (where snow density is 0.246 g cm^{-3})[51], and set 2 cm as the criterion for determining whether snow cover provides thermal insulation. Specifically, we defined SCF as the proportion of days with snow depth greater than 2 cm during periods with FDDs[4].

$$\mathrm{SCF} = \frac{\text{Days (FDD} > 0 \text{ and snow depth} > 2\text{ cm)}}{\text{Days (FDD} > 0\text{)}}. \quad (5)$$

For example, a SCF value of 0.05 indicates that 5% of freezing days coincide with a snow depth greater than 2 cm. To represent croplands with limited snow influences, we (1) tested different SCF thresholds (for example, SCF >0.05 and SCF >0.1), (2) applied a threshold of 10 cm for the minimum cumulative SWE and (3) used a threshold of 10 cm for snow depth. Supplementary Figs. 25–27 compare the sensitivities of winter wheat yield to snow droughts under various thresholds using the US observational datasets for the period of 1980–2023. These results indicate increasing sensitivity of winter wheat yield to snow droughts under various thresholds, demonstrating the robustness of our analysis. Therefore, we excluded croplands with minimal snow influence (SCF <0.05), focusing specifically on the short-term crop yield responses to snow anomalies.

Seasonality and long-term trends were removed to obtain the anomaly for each yield and climate extreme index by subtracting the long-term mean monthly signals and by applying a locally weighted scatterplot smoothing regression. Locally weighted scatterplot smoothing regression is a well-known detrending method for studying crop–climate interactions[20,37], commonly used to remove the long-term effects of technological improvements (Supplementary Text 2). By using this method, we excluded long-term trends resulting from changes in the equilibrium state, such as long-term successional cycles and frequent human management.

Detection of causal relationships between winter wheat yields and snow droughts

CCM is a powerful method that can help distinguish causality from spurious correlation in time series of nonlinear dynamical systems[21,46]. In CCM, causality is detected by measuring the extent to which the sign of the affected variable Y (yield anomalies) reliably estimates the states of a causal variable X (SWEI). That is, if variable SWEI influences winter wheat yield, then, according to the generalized Takens' theorem[21], the causal variable SWEI can be reconstructed from the historical record of the affected yield variable. The skill of cross mapping is defined as the coefficient (ρ) of the Pearson correlation between predictions and observations of SWEI. If the ρ increases with the length of time series and convergence is present, then the causal effect of SWEI on yields can be inferred.

The nonlinear Granger causality test[22] is a widely used method for investigating climate–ecosystem response by testing for causal inference in temporal data. If SWEI = (SWEI_1, SWEI_2, …, SWEI_N) and yield = (yield_1, yield_2, …, yield_N) represent the information set, where N is the length of the time series, this approach assumed that SWEI causes yield if the autoregressive forecast of yield improves when information about SWEI is included. We used the coefficient of determination (R^2) to identify Granger causality, which can be estimated as the fraction of variance explained by the forecasting model.

Yield sensitivity to snow drought

Winter wheat yields are affected not only by snow droughts but also by the occurrence of soil droughts, freezing stress, spring frosts, and severe heats[5]. To examine the sensitivity of winter wheat yield to snow anomalies, we first trained tree-based machine learning models, XGBoost[24], to explore the nonlinear sensitivities of winter wheat yield to snow drought. Then we employed explainable machine learning (SHAP) to isolate the contribution of snow anomalies to yield anomalies from the influence of other climate extremes stress (Supplementary Fig. 7). Specifically, we split the data into training (90%) and test (10%) sets. In the training set, Optuna was used to optimize the model parameters. Fivefold time series cross-validation was employed, with 90% of the data used for training and 10% for validation, using root mean square error as the fitness function. The models were trained 100 rounds to determine the optimal parameter combinations. After training, the best model and its parameters were used for prediction on each region. These algorithms are distinguished by their enhanced model accuracy and generalizability, achieved through mitigating variance and bias, consequently reducing the propensity for overfitting[52].

The XGBoost model is compatible with the SHAP method (XGB-SHAP), enabling a robust interpretation of model outputs. SHAP[23] is a game theoretic approach to explain the outputs of the XGBoost model by accounting for contributions of snowpack conditions to the winter wheat yield prediction. We treated the yield anomaly as the target variable, with the corresponding seasonal climate extreme indices as predictors, including seasonal anomalies of GDD, EDD, FDD, DrySpell, Max.5D rain and SWEI. To explore the possible influence of regional climate conditions, we built four distinct XGB-SHAP models for the four croplands: the USA, Europe, Central Asia and Eastern Asia.

For each XGB-SHAP model, we employed the SHAP dependence method to isolate the marginal contributions of SWEI on the yield anomaly. A larger negative SHAP value indicates a higher probability of yield loss, and vice versa. We defined the sensitivity as the slope estimated from the piecewise linear approach[25] between SHAP values for SWEI and SWEI values, with a breakpoint at SWEI of 0. We assumed that the grid-level interaction between yield anomaly and SWEI <0 is nearly linear. It is important to note that because sensitivity is inferred through linear regression, it may not capture the entirety of the interactions between yield and SWEI for each grid cell. In addition, to quantify interaction effects of snow and other variables, SHAP values were subsequently decomposed into main effect and interaction effect values for each feature[23]. The SHAP interaction value depicts the effects of other hydroclimatic variables on snow–yield relationships. This method combines the benefits of bootstrap aggregating and non-distribution assumption through XGBoost modelling, as well as the advantages of global interpretations being consistent with the local explanations in the SHAP algorithm, hence strengthening the robustness of the results than using traditional statistical methods[52].

Trends in sensitivity of winter wheat yield to snow drought

Grids with non-significant ($P \geq 0.1$) overall sensitivities are defined as non-snow-controlled regions. We excluded non-significant grid cells ($P \geq 0.1$) for studying changes in crop–snow relationships. To address temporal variations in winter wheat yield sensitivity to snow drought, we split the SHAP data from the entire 1982–2016 period into 25 10-year blocks (1982–1992, 1983–1993, …, 2006–2016). We assumed that the interaction between yield anomalies and reduced snow conditions at the grid level within 10-year blocks was nearly linear (Supplementary Fig. 7). We defined the slope of trends in sensitivity (T_{sen}) estimated from the Theil–Sen regression. We also used the Mann–Kendall's test to detect the statistical significance of T_{sen}.

Attribution analysis

To understand changes in T_{sen}, we used the XGB-SHAP model to predict the T_{sen}. We treated the T_{sen} as the target variable, and multiple relevant hydroclimatic trends (that is, GDD, EDD, FDD, DrySpell, Max.5D rain, T, Pre, SCF, VPD and SM) and human management practices as predictors. Human management practices include irrigation ratios, fertilizer application rates (nitrogen, phosphorus and potassium) and variations in soil types (sand and clay). We then employed SHAP values to quantify the marginal contributions of each individual factor's trends on T_{sen} and ranked the variable importance by the sum of absolute contributions across the four croplands.

Reporting summary

Further information on research design is available in the Nature Portfolio Reporting Summary linked to this article.

Data availability

All data used in this study are puWe defined an increasing trendbal Dataset of Historical Yield of winter wheat yields are available at https://sage.nelson.wisc.edu/data-and-models/datasets/crop-calendar-dataset/ and https://doi.org/10.1594/PANGAEA.909132. Yearly county-level yields and key phenology dates for winter wheat in the USA were obtained from USDA NASS QuickStats (https://quickstats.nass.usda.gov/). Phenology stages for winter wheat in France were obtained from France AgriMer (https://cereobs.franceagrimer.fr/cereobs-sp/#/). Hourly 2-m air temperatures, daily precipitation and dew point temperature were obtained from ERA5-Land reanalysis datasets (https://cds.climate.copernicus.eu/cdsapp#!/dataset/reanalysis-era5-land?tab=overview). The daily snow depth water equivalent and snow depth were obtained from the ERA5-Land reanalysis datasets (https://cds.climate.copernicus.eu/cdsapp#!/dataset/reanalysis-era5-land?tab=overview) and the GLDAS Catchment Land Surface Model L4.0 (https://disc.gsfc.nasa.gov/datasets/GLDAS_CLSM025_D_2.0/summary?keywords=GLDAS). Daily root-zone soil moisture was obtained from the GLEAM dataset (https://www.gleam.eu/). The datasets used to reproduce the methods and findings of this study are available via Zenodo at https://doi.org/10.5281/zenodo.17861863 (ref. 53).

Code availability

The code used for this study is available via Zenodo at https://doi.org/10.5281/zenodo.17861863 (ref. 53).

References

1. Ombadi, M., Risser, M. D., Rhoades, A. M. & Varadharajan, C. A warming-induced reduction in snow fraction amplifies rainfall extremes. *Nature* **619**, 305–310 (2023).
2. Qin, Y. et al. Agricultural risks from changing snowmelt. *Nat. Clim. Change* **10**, 459–465 (2020).
3. Qin, Y. et al. Snowmelt risk telecouplings for irrigated agriculture. *Nat. Clim. Change* **12**, 1007–1015 (2022).
4. Zhu, P. et al. The critical benefits of snowpack insulation and snowmelt for winter wheat productivity. *Nat. Clim. Change* **12**, 485–490 (2022).
5. Trnka, M. et al. Adverse weather conditions for European wheat production will become more frequent with climate change. *Nat. Clim. Change* **4**, 637–643 (2014).
6. Huning, L. S. & AghaKouchak, A. Global snow drought hot spots and characteristics. *Proc. Natl Acad. Sci. USA* **117**, 19753–19759 (2020).
7. Gottlieb, A. R. & Mankin, J. S. Observing, measuring, and assessing the consequences of snow drought. *Bull. Am. Meteorol. Soc.* **103**, E1041–E1060 (2022).
8. Howitt, R. E., Medellín-Azuara, J., Macewan, D., Lund, J. R. & Sumner, D. A. *Economic Impact of the 2015 Drought on Farm Revenue and Employment* (University of California Giannini Foundation of Agricultural Economics, 2015).
9. Seager, R. et al. Mechanisms of a meteorological drought onset: summer 2020 to spring 2021 in southwestern North America. *J. Clim.* **35**, 7367–7385 (2022).
10. Farmers grappling with Afghanistan drought urgently need seed and animal feed support. *FAO* https://www.fao.org/newsroom/detail/Farmers-grappling-with-Afghanistan-drought-urgently-need-seed-and-animal-feed-support/en (2018).
11. Colombo, N. et al. Unprecedented snow-drought conditions in the Italian Alps during the early 2020s. *Environ. Res. Lett.* **18**, 074014 (2023).
12. AghaKouchak, A. et al. Toward impact-based monitoring of drought and its cascading hazards. *Nat. Rev. Earth Environ.* **4**, 582–595 (2023).
13. Kraaijenbrink, P. D. A., Stigter, E. E., Yao, T. & Immerzeel, W. W. Climate change decisive for Asia's snow meltwater supply. *Nat. Clim. Change* **11**, 591–597 (2021).
14. Lutz, A. F. et al. South Asian agriculture increasingly dependent on meltwater and groundwater. *Nat Clim. Change* **12**, 566–573 (2022).
15. Musselman, K. N., Addor, N., Vano, J. A. & Molotch, N. P. Winter melt trends portend widespread declines in snow water resources. *Nat. Clim. Change* **11**, 418–424 (2021).
16. Li, X. & Wang, S. Recent increase in the occurrence of snow droughts followed by extreme heatwaves in a warmer world. *Geophys. Res. Lett.* **49**, 1–10 (2022).
17. Proctor, J., Rigden, A., Chan, D. & Huybers, P. More accurate specification of water supply shows its importance for global crop production. *Nat. Food* **3**, 753–763 (2022).
18. Hersbach, H. et al. The ERA5 global reanalysis. *Q. J. R. Meteorol. Soc.* **146**, 1999–2049 (2020).
19. Rodell, M. et al. The global land data assimilation system. *Bull. Am. Meteorol. Soc.* **85**, 381–394 (2004).
20. Ben-Ari, T. et al. Causes and implications of the unforeseen 2016 extreme yield loss in the breadbasket of France. *Nat. Commun.* **9**, 1627 (2018).
21. Sugihara, G. et al. Detecting causality in complex ecosystems. *Science* **338**, 496–500 (2012).
22. Granger, C. W. J. Investigating causal relations by econometric models and cross-spectral methods. *Econometrica* **37**, 424–438 (1969).
23. Lundberg, S. M. et al. From local explanations to global understanding with explainable AI for trees. *Nat. Mach. Intell.* **2**, 56–67 (2020).
24. Chen, T. & Guestrin, C. Xgboost: a scalable tree boosting system. In *Proc. 22nd ACM SIGKDD International Conference on Knowledge Discovery and Data Mining* 785–794 (Association for Computing Machinery, 2016).
25. Bönecke, E. et al. Decoupling of impact factors reveals the response of German winter wheat yields to climatic changes. *Glob. Change Biol.* **26**, 3601–3626 (2020).

26. Wang, R. et al. Winter dormant wheat will benefit from mean temperature increase of 2 °C when well-watered and fertilized in the main producing regions of China. *Glob. Change Biol.* **31**, e70324 (2025).
27. Vico, G., Hurry, V. & Weih, M. Snowed in for survival: quantifying the risk of winter damage to overwintering field crops in northern temperate latitudes. *Agric. For. Meteorol.* **197**, 65–75 (2014).
28. Vogel, F. A. & Bange, G. A. *Understanding USDA Crop Forecasts* (USDA, 1999).
29. Edwards, A. C., Scalenghe, R. & Freppaz, M. Changes in the seasonal snow cover of alpine regions and its effect on soil processes: a review. *Quat. Int.* **162**, 172–181 (2007).
30. Yakutina, O. P., Nechaeva, T. V. & Smirnova, N. V. Consequences of snowmelt erosion: soil fertility, productivity and quality of wheat on Greyzemic Phaeozem in the south of West Siberia. *Agric. Ecosyst. Environ.* **200**, 88–93 (2015).
31. Siirila-Woodburn, E. R. et al. A low-to-no snow future and its impacts on water resources in the western United States. *Nat. Rev. Earth Environ.* **2**, 800–819 (2021).
32. Sloat, L. L. et al. Climate adaptation by crop migration. *Nat. Commun.* **11**, 1243 (2020).
33. Wang, Y., Shi, W. & Wen, T. Prediction of winter wheat yield and dry matter in North China Plain using machine learning algorithms for optimal water and nitrogen application. *Agric. Water. Manag.* **277**, 108140 (2023).
34. Zhang, T. et al. Climate change may outpace current wheat breeding yield improvements in North America. *Nat. Commun.* **13**, 5591 (2022).
35. Lv, L. et al. Winter wheat grain yield and its components in the North China Plain: irrigation management, cultivation, and climate. *Chil. J. Agric. Res.* **73**, 233–242 (2013).
36. Iizumi, T. & Sakai, T. The global dataset of historical yields for major crops 1981–2016. *Sci. Data* **7**, 1–7 (2020).
37. Chen, H. & Wang, S. Compound dry and wet extremes lead to an increased risk of rice yield loss. *Geophys. Res. Lett.* https://doi.org/10.1029/2023GL105817 (2023).
38. Quick Stats tools. *USDA* https://www.nass.usda.gov/Quick_Stats/ (2025).
39. *FranceAgriMar* https://cereobs.franceagrimer.fr/cereobs-sp/#/ (2025).
40. Lobert, F. et al. A deep learning approach for deriving winter wheat phenology from optical and SAR time series at field level. *Remote Sens. Environ.* **298**, 113800 (2023).
41. Zhang, Q. J., Wu, D. L. & Gao, J. Variation of winter wheat phenology dataset in Huang Huai Hai Plain of China from 1981 to 2021. *Sci. Data* **12**, 1203 (2025).
42. Liao, C. et al. Near real-time detection and forecasting of within-field phenology of winter wheat and corn using Sentinel-2 time-series data. *ISPRS J. Photogramm. Remote Sens.* **196**, 105–119 (2023).
43. Yu, Q. et al. A cultivated planet in 2010–part 2: the global gridded agricultural-production maps. *Earth Syst. Sci. Data* **12**, 3545–3572 (2020).
44. Mueller, N. D. et al. Closing yield gaps through nutrient and water management. *Nature* **490**, 254–257 (2012).
45. Martens, B. et al. GLEAM v3: satellite-based land evaporation and root-zone soil moisture. *Geosci. Model Dev.* **10**, 1903–1925 (2017).
46. Qing, Y. et al. Accelerated soil drying linked to increasing evaporative demand in wet regions. *npj Clim. Atmos. Sci.* **6**, 205 (2023).
47. Tack, J., Barkley, A. & Nalley, L. L. Effect of warming temperatures on US wheat yields. *Proc. Natl Acad. Sci. USA* **112**, 6931–6936 (2015).
48. Troy, T. J., Kipgen, C. & Pal, I. The impact of climate extremes and irrigation on US crop yields. *Environ. Res. Lett.* https://doi.org/10.1088/1748-9326/10/5/054013 (2015).
49. Sacks, W. J., Deryng, D., Foley, J. A. & Ramankutty, N. Crop planting dates: an analysis of global patterns. *Glob. Ecol. Biogeogr.* **19**, 607–620 (2010).
50. Ge, X. et al. Effects of canopy composition on snow depth and below-the-snow temperature regimes in the temperate secondary forest ecosystem, Northeast China. *Agric. For. Meteorol.* **313**, 108744 (2022).
51. Zhao, W. et al. Spatial and temporal variability in snow density across the Northern Hemisphere. *Catena* **232**, 107445 (2023).
52. Li, W. et al. Widespread increasing vegetation sensitivity to soil moisture. *Nat. Commun.* **13**, 3959 (2022).
53. Huijiao, C. Winter wheat yield sensitivity to snow drought is increasing across the Northern Hemisphere. *Zenodo* https://doi.org/10.5281/zenodo.17861863 (2025).

Acknowledgements

The work described in this article was supported by a grant from the Research Grants Council of the Hong Kong Special Administrative Region, China (project no. PolyU/RGC 15232023), the Otto Poon Research Institute for Climate-Resilient Infrastructure (project no. P0055919) and the State Key Laboratory of Climate Resilience for Coastal Cities at the Hong Kong Polytechnic University.

Author contributions

H.C. and S.W. designed the study. H.C. carried out the analysis and drafted the paper. S.W. supervised the analysis and contributed to the interpretation and discussion of the results. P.Z. and A.A. provided comments and suggestions for improving the quality of this paper. All authors edited the paper.

Competing interests

The authors declare no competing interests.

Additional information

Supplementary information The online version contains supplementary material available at https://doi.org/10.1038/s43016-026-01302-7.

Correspondence and requests for materials should be addressed to Shuo Wang.

Peer review information *Nature Food* thanks Jarrod Kath, Giulia Vico, Wei Xiong and the other, anonymous, reviewer(s) for their contribution to the peer review of this work.

nature portfolio

Corresponding author(s): Shuo Wang

Last updated by author(s): Dec 16, 2025

Reporting Summary

Nature Portfolio wishes to improve the reproducibility of the work that we publish. This form provides structure for consistency and transparency in reporting. For further information on Nature Portfolio policies, see our Editorial Policies and the Editorial Policy Checklist.

Statistics

For all statistical analyses, confirm that the following items are present in the figure legend, table legend, main text, or Methods section.

n/a	Confirmed
☐	☒ The exact sample size (*n*) for each experimental group/condition, given as a discrete number and unit of measurement
☐	☒ A statement on whether measurements were taken from distinct samples or whether the same sample was measured repeatedly
☐	☒ The statistical test(s) used AND whether they are one- or two-sided *Only common tests should be described solely by name; describe more complex techniques in the Methods section.*
☐	☒ A description of all covariates tested
☐	☒ A description of any assumptions or corrections, such as tests of normality and adjustment for multiple comparisons
☐	☒ A full description of the statistical parameters including central tendency (e.g. means) or other basic estimates (e.g. regression coefficient) AND variation (e.g. standard deviation) or associated estimates of uncertainty (e.g. confidence intervals)
☐	☒ For null hypothesis testing, the test statistic (e.g. *F*, *t*, *r*) with confidence intervals, effect sizes, degrees of freedom and *P* value noted *Give P values as exact values whenever suitable.*
☒	☐ For Bayesian analysis, information on the choice of priors and Markov chain Monte Carlo settings
☐	☒ For hierarchical and complex designs, identification of the appropriate level for tests and full reporting of outcomes
☐	☒ Estimates of effect sizes (e.g. Cohen's *d*, Pearson's *r*), indicating how they were calculated

Our web collection on statistics for biologists contains articles on many of the points above.

Software and code

Policy information about availability of computer code

Data collection	No software was used.
Data analysis	Our analyses were performed using R verson 4.4.1 and Python version 3.12, with the codes available from https://doi.org/10.5281/zenodo.17861863

For manuscripts utilizing custom algorithms or software that are central to the research but not yet described in published literature, software must be made available to editors and reviewers. We strongly encourage code deposition in a community repository (e.g. GitHub). See the Nature Portfolio guidelines for submitting code & software for further information.

Data

Policy information about availability of data

All manuscripts must include a data availability statement. This statement should provide the following information, where applicable:

- Accession codes, unique identifiers, or web links for publicly available datasets
- A description of any restrictions on data availability
- For clinical datasets or third party data, please ensure that the statement adheres to our policy

The Crop Calendar and the Global Dataset of Historical Yield of winter wheat yields were accessible through https://sage.nelson.wisc.edu/data-and-models/datasets/crop-calendar-dataset/ and https://doi.org/10.1594/PANGAEA.909132. Yearly county-level winter wheat yields were obtained from USDA NASS QuickStats (https://quickstats.nass.usda.gov/). Phenology dates for winter wheat in the United States were obtained from USDA NASS QuickStats (https://

quickstats.nass.usda.gov/). Phenology stages for winter wheat in France were obtained from France AgriMer (https://cereobs.franceagrimer.fr/cereobs-sp/#/). Hourly 2-m air temperatures, daily precipitation, and dew point temperature were obtained from ERA5-Land reanalysis datasets https://cds.climate.copernicus.eu/cdsapp#!/dataset/reanalysis-era5-land?tab=overview. The daily snow depth water equivalent and snow depth were obtained from the ERA5-Land reanalysis datasets https://cds.climate.copernicus.eu/cdsapp#!/dataset/reanalysis-era5-land?tab=overview and the GLDAS Catchment Land Surface Model L4.0 https://disc.gsfc.nasa.gov/datasets/GLDAS_CLSM025_D_2.0/summary?keywords=GLDAS . Daily root-zone soil moisture was obtained from the Global Land Evaporation Amsterdam Model (GLEAM) dataset https://www.gleam.eu/.

Research involving human participants, their data, or biological material

Policy information about studies with human participants or human data. See also policy information about sex, gender (identity/presentation), and sexual orientation and race, ethnicity and racism.

Reporting on sex and gender	N.A.
Reporting on race, ethnicity, or other socially relevant groupings	N.A.
Population characteristics	N.A.
Recruitment	N.A.
Ethics oversight	N.A.

Note that full information on the approval of the study protocol must also be provided in the manuscript.

Field-specific reporting

Please select the one below that is the best fit for your research. If you are not sure, read the appropriate sections before making your selection.

☐ Life sciences ☐ Behavioural & social sciences ☒ Ecological, evolutionary & environmental sciences

For a reference copy of the document with all sections, see nature.com/documents/nr-reporting-summary-flat.pdf

Ecological, evolutionary & environmental sciences study design

All studies must disclose on these points even when the disclosure is negative.

Study description	We used two long-term snow datasets and two winter wheat yield datasets to explore the hotspot and trends of snow drought impacts on wheat wheat yield in the global key winter wheat-producing regions. We also explore the underlying mechanisms behind the increasing sensitivity of winter wheat yield to snow droughts.
Research sample	Global gridded winter wheat yield were obtained from the GHDY dataset. The observational yearly county-level winter wheat yield were assessed from USDA NASS database. Global gridded daily snow depth water equivalent and snow depth, 2-m air temperature, precipitation, and dew point temperature were obtained from ERA5-Land and GLDAS datasets.Daily root-zone soil moisture was obtained from the GLEAM dataset.
Sampling strategy	We used all available samples.
Data collection	The Crop Calendar and the Global Dataset of Historical Yield of winter wheat yields were accessible through https://sage.nelson.wisc.edu/data-and-models/datasets/crop-calendar-dataset/ and https://doi.org/10.1594/PANGAEA.909132. Yearly county-level yields and phenology dates for winter wheat in the United States were obtained from USDA NASS QuickStats (https://quickstats.nass.usda.gov/). Phenology stages for winter wheat in France were obtained from France AgriMer (https://cereobs.franceagrimer.fr/cereobs-sp/#/). Hourly 2-m air temperatures, daily precipitation, and dew point temperature were obtained from ERA5-Land reanalysis datasets https://cds.climate.copernicus.eu/cdsapp#!/dataset/reanalysis-era5-land?tab=overview. The daily snow depth water equivalent was obtained from the ERA5-Land reanalysis datasets https://cds.climate.copernicus.eu/cdsapp#!/dataset/reanalysis-era5-land?tab=overview and the GLDAS Catchment Land Surface Model L4.0 https://disc.gsfc.nasa.gov/datasets/GLDAS_CLSM025_D_2.0/summary?keywords=GLDAS . Daily root-zone soil moisture was obtained from the Global Land Evaporation Amsterdam Model (GLEAM) dataset https://www.gleam.eu/.
Timing and spatial scale	Hotspot and the trend of snow droughts across global winter wheat croplands for the period of 1960-2020. The trends of sensitivity of winter wheat yield to snow droughts was conducted from 1982 to 2016 across global winter wheat producing region. The snow drought effects on winter wheat yield in the United States was conducted from 1980-2023.
Data exclusions	No data was excluded
Reproducibility	Our results can be reproduced when following the described methods and input data set.

Randomization	This is not relevant to our study.
Blinding	This is not relevant to our study.

Did the study involve field work? ☐ Yes ☒ No

Reporting for specific materials, systems and methods

We require information from authors about some types of materials, experimental systems and methods used in many studies. Here, indicate whether each material, system or method listed is relevant to your study. If you are not sure if a list item applies to your research, read the appropriate section before selecting a response.

Materials & experimental systems

n/a	Involved in the study
☒	☐ Antibodies
☒	☐ Eukaryotic cell lines
☒	☐ Palaeontology and archaeology
☒	☐ Animals and other organisms
☒	☐ Clinical data
☒	☐ Dual use research of concern
☒	☐ Plants

Methods

n/a	Involved in the study
☒	☐ ChIP-seq
☒	☐ Flow cytometry
☒	☐ MRI-based neuroimaging

Plants

Seed stocks	N.A.
Novel plant genotypes	N.A.
Authentication	N.A.